



Published in final edited form as:

Medchemcomm. 2012 August ; 3(8): 987–996. doi:10.1039/C2MD20029E.

Comparative analysis of the biosynthetic systems for fungal bicyclo[2.2.2]diazaoctane indole alkaloids: the (+)/(–)-notoamide, paraherquamide and malbrancheamide pathways

Shengying Li^a, Krithika Anand^a, Hong Tran^a, Fengan Yu^a, Jennifer M. Finefield^b, James D. Sunderhaus^b, Timothy J. McAfoos^b, Sachiko Tsukamoto^c, Robert M. Williams^{b,d}, and David H. Sherman^{a,e}

Robert M. Williams: rmw@lamar.colostate.edu; David H. Sherman: davidhs@umich.edu

^aLife Sciences Institute, University of Michigan, Ann Arbor, Michigan 48109, USA

^bDepartment of Chemistry, Colorado State University, Fort Collins, Colorado 80523

^cGraduate School of Pharmaceutical Sciences, Kumamoto University, 5-1 Oe-honmachi, Kumamoto 862-0973, Japan

^dUniversity of Colorado Cancer Center, Aurora, Colorado 80045, USA

^eDepartments of Medicinal Chemistry, Microbiology & Immunology, and Chemistry, University of Michigan, Ann Arbor, Michigan 48109, USA

Abstract

The biosynthesis of fungal bicyclo[2.2.2]diazaoctane indole alkaloids with a wide spectrum of biological activities have attracted increasing interest. Their intriguing mode of assembly has long been proposed to feature a non-ribosomal peptide synthetase, a presumed intramolecular Diels-Alderase, a variant number of prenyltransferases, and a series of oxidases responsible for the diverse tailoring modifications of their cyclodipeptide-based structural core. Until recently, the details of these biosynthetic pathways have remained largely unknown due to lack of information on the fungal derived biosynthetic gene clusters. Herein, we report a comparative analysis of four natural product metabolic systems of a select group of bicyclo[2.2.2]diazaoctane indole alkaloids including (+)/(–)-notoamide, paraherquamide and malbrancheamide, in which we propose an enzyme for each step in the biosynthetic pathway based on deep annotation and on-going biochemical studies.

Introduction

Natural products continue to be a rich source of clinical drugs for treatment of human and animal diseases.^{1, 2} With respect to drug development, advanced understanding of their biosynthesis is significant for rational strain improvement efforts. This includes genetic manipulation (e.g. gene knock-out, knock-in, and whole gene cluster amplification) of the key biosynthetic and regulatory genes in order to increase the yield of pharmaceuticals to a desired level.^{3–6} Knowledge on biosynthesis is also valuable for guiding generation of novel natural product analogs as new drug candidates by metabolic engineering, mutasynthesis and allied approaches.^{7–11} In addition, biochemical characterization of diverse biosynthetic enzymes continues to reveal new catalytic mechanisms that inspire inventions of novel chemical and biological catalysts in organic chemistry for production of fine-chemical and medicinal agents.^{12,13}

Elucidation of the biosynthetic pathway of a particular natural product or a family of natural products first requires identification of the gene cluster encoding its production.^{14–16} Next, the combined genetic (*in vivo*) and biochemical characterization (*in vitro*) of each individual biosynthetic enzyme provides important information, including enzyme substrate specificity, cofactor requirements, and the precise order of multiple biosynthetic steps.^{17,18} With this information available, it becomes possible to reconstitute the entire biosynthetic pathway in a heterologous host^{19–21} or in a multi-component *in vitro* reaction.^{22, 23}

Across all microbes, plants and animals that generate natural products, it is particularly challenging to elucidate a biosynthetic pathway completely when unprecedented steps are involved, or precedent knowledge of biosynthetic origin is limited or non-existent. Conventionally, the hunting for such enzymes catalyzing these unusual biotransformations via unexplored mechanisms depends on implementing reasonable biosynthetic principles, and the scanning of the activity of all possible candidate enzymes against all hypothetical substrates.^{18,24,25} Thus, the entire process can require prolonged and intensive efforts, especially for those complex natural products assembled by a large number of biosynthetic enzymes.

Due to the discovery of natural products from different microorganisms bearing the same unique structural core, but varying from one another in their tailoring groups, opportunities for facile identification of unique enzymes arise. In this scenario comparative bioinformatic analysis suggests that homologous genes can be linked to formation of a common structural core, whereas cluster-specific genes provide the basis for structural differences.^{26–29} Recent advances in whole genome sequencing technology have made this approach rapid and cost-effective.^{30–34} Thus, identification of biosynthetic gene clusters for structurally related natural products from different microorganisms has become practical for comparative analysis of these systems. Deep annotation provides adequate information to develop hypotheses regarding key gene(s) and their protein products. This in turn guides experimental strategies to explore unusual biotransformation(s) of interest using genetic and/or biochemical approaches. Although considerable information can be gleaned from biosynthetic pathway mining and annotation, putative biochemical function can only be verified by analysis of the gene product *in vitro* using natural or suitable model substrates.

Herein, we present an example of the comparative analysis of biosynthetic gene clusters (mined from the whole genome) and pathways for four structurally related fungal indole alkaloids bearing the unusual bicyclo[2.2.2]diazaoctane core, including the anticancer agents (–)-notoamide A ((–)-**1**) and (+)-notoamide A ((+)-**1**),^{35, 36} the anthelmintic paraherquamide A (**2**),^{37–39} and the calmodulin-inhibitor malbrancheamide^{40–42} (**3**) (Fig. 1A) produced by *Aspergillus* sp. MF297-2,⁴³ *Aspergillus versicolor* NRRL35600, *Penicillium fellutanum* ATCC20841, and *Malbranchea aurantiaca* RRC1813, respectively. These fungal natural products are assembled from an L-tryptophan, a second cyclic amino acid residue, and one or two isoprene units through biosynthetic pathways that are proposed to feature an intriguing intramolecular Diels Alderase (IMDAse), and a number of unique enantiomerically selective enzymes.^{44–49} The diverse bioactivities of this natural product family suggests that elucidation of their biosynthesis could direct future structural diversification via biosynthetic engineering, thereby leading to enhanced biological activities.

As expected, this comparative analysis provides significant insights into a number of intriguing biosynthetic questions: (1) which enzyme in each pathway is likely responsible for the formation of the bicyclo[2.2.2]diazaoctane core via the proposed intramolecular [4+2] Diels-Alder (IMDA) cyclization; (2) which enzyme in the pathway of **1** and **2** installs the *spiro*-oxindole functionality via a putative epoxide-initiated Pinacol-type rearrangement;

and (3) what genetic difference controls formation of the dioxopiperazine in **1** versus the monooxopiperazine in **2** and **3**.

Results and discussion

Structural similarity between 1–3 and its biosynthetic implications

The most significant structural similarity between **1–3** is the bicyclo[2.2.2]diazaoctane core (Fig. 1A). Biosynthetically, this unique structural moiety was proposed to arise from a [4+2] IMDA reaction (Fig. 1B).^{44, 46} This presumed cycloaddition reaction is also believed to catalyze the first enantiodivergent step in an otherwise common biosynthetic pathway from *Aspergillus* sp. MF297-2 and *A. versicolor* NRRL35600, leading to formation of (–)-**1** and (+)-**1**, respectively, together with several other enantiomeric metabolites (Fig. 3).⁴⁷ Currently, it remains unknown whether a specific IMDase indeed exists in these biosynthetic pathways. However, if it does exist, one would expect its encoding gene should be present in all four gene clusters. Second, the *spiro*-oxindole is absent in **3**, suggesting the responsible enzyme is likely absent from the pathway for **3**, and present in those for **1** and **2**. Third, a specific reductase responsible for reducing the tryptophan carbonyl group would be expected in the gene cluster of **2** and **3**, but not **1**. This genetic difference would account for the lack of the second amide carbonyl group in the piperazine ring of **2** and **3**. Finally, the different hydroxylation status of the indole amide, distinct aromatic decoration among **1–3**, together with other unique structural features including the tailoring of the proline moiety and *N*-methylation in **2**, are also expected to be reflected at the genetic level.

Localization and analysis of the gene clusters of (–)-notoamide (*not*), (+)-notoamide (*not'*), paraherquamide (*phq*), and malbrancheamide (*mal*) through genome mining

The genomes of *A. versicolor* NRRL35600, *P. fellutanum* ATCC20841, and *M. aurantiaca* RRC1813A harboring *not'*, *phq*, and *mal* gene clusters, respectively were sequenced to approximately 99, 84, and 181 times coverage of their estimated genome size (35 Mb), using the Illumina Solexa technology (Genome Analyzer IIx).

First, the key biosynthetic gene *notE'* (Table 1) encoding a non-ribosomal peptide synthetase (NRPS) was mined from the genome sequences using the *notE* DNA sequence from the reported *not* gene cluster⁴³ as a probe for homologous genes. NotE', which shows 79% identity and 86% similarity to NotE at the amino acid (AA) level, was predicted to be a bimodular NRPS with the A-T-C-A-T-C (A: adenylation, T: thiolation, C: condensation) domain organization using the PKS/NRPS Analyzer (<http://nrps.igs.umaryland.edu/nrps/>). Genome walking from *notE'* toward 5' and 3' ends identified another nine genes (*notA'-J'*, Table 1 and Fig. 2) that display high AA sequence similarity (>70%) with corresponding gene products of the *not* gene cluster. Notably, the overall nucleotide identity between *notA'-J'* (25,440 bp) and *notA-J* (26,210 bp) is 71%, which is not surprising since both metabolic pathways are responsible for assembling “identical”, yet antipodal compounds. In addition to the high sequence similarity, the genetic architecture (i.e. order and direction of genes) within this region is identical in the two clusters (Fig. 2). The pattern of the exon/intron arrangement in the corresponding genes is also highly similar to each other (see Supplementary Information). In contrast, the sequence similarity is reduced drastically and the gene architecture differs after *notK'/notK* (Table 1, Fig. 2), strongly suggesting the previously assigned *not* gene cluster (*notA-R*) probably ends at *notJ*.

At the genetic level, it is not possible to glean the key differences that account for production of antipodal notoamide metabolites, suggesting that subtle active site sequence variation in those enantiomerically selective enzymes play a critical role in the control of absolute chirality. This requires direct biochemical analysis of the key notoamide

biosynthetic enzymes, including structural biology efforts, which is currently ongoing in our laboratories.

Second, the paraherquamide (*phq*) gene cluster (47,884 bp) was identified from the partially assembled *P. fellutanum* genome by using a select group of *not* genes including the NRPS gene *notE*, the prenyltransferase genes *notC* and *notF*, and the P450 monooxygenase gene *notG* as *in silico* probes.⁴³ Fifteen genes were identified that are likely involved in paraherquamide biosynthesis. The largest number of biosynthetic genes among the four studied metabolic pathways is consistent with **2** as the most complex structure compared to **1** and **3**. Comparative bioinformatic analysis demonstrates that nine (*phqA*, *B*, *F*, *G*, *H*, *J*, *K*, *L*, and *M*) out of fifteen total *phq* genes are homologous to corresponding *not* genes (Table 1), although their homology is significantly lower than that between *not* and *not'* genes. Notably, the bimodular *phqB* NRPS gene is different from *notE* in that a reductase (R) domain is located at its carboxy terminus instead of a condensation (C) domain, which is found in *notE* and *notE'*. This difference is significant because the reductase (*vs* condensation) domain is presumed to account for the presence of the monooxopiperazine in **2** (*vs* dioxopiperazine in **1**) (see below).⁵⁰ Among the remaining six cluster-specific genes, *phqC* shows high sequence similarity to 2-oxoglutarate (2OG) and Fe(II) dependent oxygenases.^{51,52} The *phqD* and *phqE* genes, which putatively encoding a pyrroline-5-carboxylate reductase and a short chain dehydrogenase, respectively, might be involved in the formation of the β -methyl-proline starter unit. The *phqI* gene that encodes the third prenyltransferase in *phq* is unique as it is free of introns, and therefore, distinct from the single intron-containing prenyltransferase genes *phqA/notC* and *phqJ/notF*. It is worth noting that the presence of three prenyltransferase genes is inconsistent with the two isoprene groups incorporated into the structure of **2**. Thus, it is of special interest to examine whether the third prenyltransferase gene is redundant or plays an alternative, and as yet unknown function in the biosynthesis of **2**. Furthermore, *phqN* is predicted to function as a methyltransferase, likely responsible for the *N*-methylation in **2**. Finally, the *phqO* P450 gene with a unique exon/intron organization pattern is hypothesized to catalyze the C14 hydroxylation of the β -methyl-proline moiety.

Third, the seven-gene containing *mal* gene cluster (20179 bp) was mined from the genome of *Malbranchea aurantiaca* RRC1813A using *phqB* as an *in silico* probe to identify the metabolic system for **3**. It has the smallest size among gene clusters of **1–3**, which is consistent with the simplest structure and corresponding biosynthetic pathway. The genes *malB*, *malD*, *malE*, *malF*, and *malG* are common to the four gene clusters. Thus, except for the regulatory gene of *malD* (homologous to *notA*, *notA'* and *phqG*), the remaining four biosynthetic genes (and their homologues in *not*, *not'* and *phq*) are possibly responsible for installing the shared structural features of **1–3**. This strongly suggests that the hypothetical Diels Alderases (if extant) should be represented by one of these four gene products (see below). Interestingly, the *mal* genes show greater sequence similarity to *phq* genes than *not* (or *not'*) genes, perhaps indicating their closer evolutionary relationship. Similar to PhqB, the NRPS MalG harbors a reductase domain at its carboxy terminus, which is consistent with the monooxopiperazine moiety in **3**. Again, the apparent redundancy of the second prenyltransferase (**3** only contains one isoprene group) is difficult to rationalize, but genetic disruption or RNA silencing (*malB* or *malE*) efforts are likely to shed light on the individual role of these enzymes. Finally, it is evident that the flavin-dependent halogenase MalA is likely involved in the introduction of one or both chlorine atoms in the biosynthesis of **3**.

Biosynthetic pathway of notoamide A ((-)-1 and (+)-1)

Since the discovery of the biosynthetic gene cluster of (-)-**1** from marine *Aspergillus* sp. MF297-2, *in vitro* biochemical characterization of the reverse prenyltransferase NotF using

the NRPS (NotE) product brevianamide F⁵³ (**4**) as substrate and the normal prenyltransferase NotC using 6-hydroxy-deoxybrevianamide E (**6**) as substrate has partially established the early steps of the notoamide pathway leading to notoamide S (**7**) (Fig. 3).⁴³ The P450 monooxygenase NotG is likely catalyzing the C6 indole hydroxylation since its close homologue FtmC (59%/72% identity/similarity) in fumitremorgin biosynthesis had been characterized to hydroxylate the analogous aromatic C-H bond in the indole ring of tryprostatin B,^{54,55} which is structurally similar to deoxybrevianamide E (**5**).⁵⁶

As the proposed pivotal branching point in notoamide biosynthesis,^{47,57,58} **7** can be diverted to notoamide E (**8**) through an oxidative pyran ring closure putatively catalyzed by either NotH P450 monooxygenase (based on precedented examples of pyran ring formation from the epoxide intermediate generated by P450 enzymes⁵⁹), or the NotD oxidoreductase. This step would be followed by an indole 2,3-epoxidation-initiated Pinacol-like rearrangement catalyzed by NotB FAD monooxygenase (FMO) leading to the formation of notoamide C (**9**) and notoamide D (**10**).⁵⁸ Notably, *notB* (or *notB'*) is only observed in the *not* (or *not'*) gene cluster, consistent with the fact that this branching pathway leading to natural products **9** and **10** is only observed in notoamide biosynthesis.

On the other hand, extensive precursor feeding and incorporation studies using stable isotopically labeled intermediates have supported **7** as the substrate for the hypothetical IMDA.⁴⁷ As a working hypothesis, a two-electron oxidation catalyzed by an oxidase would give rise to the achiral azadiene intermediate (**11**), which may immediately undergo a spontaneous stereoselective [4+2] IMDA cyclization in the active site of the same oxidase, yielding either (+)-notoamide T ((+)-**12**) in *Aspergillus* sp. MF297-2 or (-)-notoamide T ((-)-**12**) in *A. versicolor*. The opposing conformation (*endo/exo*) assumed by achiral **11** presumably determined by the scaffolding of each putative Diels-Alderase might account for the enantio-divergence at this key step. The five oxidases encoded by the *not* gene cluster, include FMO NotB and NotI, P450 enzymes NotG and NotH, and the FAD-dependent oxidoreductase NotD. NotB was recently identified as the notoamide E oxidase.⁵⁸ NotI is highly similar to NotB with 42% protein sequence identity and 59% similarity, and is predicted to catalyze a similar conversion from (+)-stephacidin A⁶⁰ ((+)-**13**) to (-)-notoamide B ((-)-**14**) via the 2,3-epoxidation of (+)-**13** followed by a Pinacol-type rearrangement. Thus, if the putative function of NotG (see above) is correct, NotH (or NotD) is likely the bifunctional oxidase that also functions as the IMDAse responsible for generation of (+)-**12**. To generate antipodal (-)-**12**, NotH' (or NotD') is expected to catalyze a Diels Alder reaction leading to the opposite stereochemistry. Currently, this hypothesis is being tested in our laboratories through *in vitro* characterization of NotH/NotH' (or NotD/NotD'). With comparative analysis of four gene clusters (Table 1), it appears that NotD/NotD' is more likely to serve as the IMDAse since its homologs (PhqH and MalF) are present in all clusters. This hypothesis is based on the assumption that these four biosynthetic pathways use the same type of protein scaffolding enzyme to catalyze the [4+2] cycloaddition. However, we have recently begun to challenge this assumption (see below). Presently, the possibility that NotH/NotH' functions as the IMDAse in notoamide biosynthesis cannot be excluded. Once its identity is determined, the final oxidase NotD (or NotH) will likely be found to catalyze the oxidative pyran ring formation (Fig. 3).

Another important fact of these two related notoamide pathways is that enzymes catalyzing the biosynthetic steps after formation of **12** must also be enantiomerically and diastereochemically selective. Specifically, in previous precursor incorporation studies of racemic ¹³C-labeled (±)-**13** with *Aspergillus* sp. MF297-2 and *A. versicolor*,⁶¹ it was ascertained that only one enantiomer of **13** can be processed (currently presumed by NotI and NotI') to form downstream products. Understanding the subtle differences between

these two enzymes will likely provide significant insights into how related enzymes have evolved to adopt opposing enantiomeric selectivity.

Finally, it remains unclear which enzyme could be responsible for the final hydroxylation steps leading to notoamide **1** and sclerotiamide⁶² (**15**) since all five oxidative enzymes in the *not*(') gene cluster has been assigned a putative function. It is possible that **1** and **15** are opportunistically produced upon the activity of unknown oxidases whose genes reside outside of the defined notoamide gene cluster. Alternatively, the possibility that a *not* oxidase may possess bi-functionality cannot be excluded.

Biosynthetic pathway of paraherquamide A (**2**)

Previous feeding studies demonstrated that L-isoleucine is the precursor to the β -methyl β -hydroxy proline moiety in **2**.^{45, 63} Identification of the pyrroline-5-carboxylate reductase PhqD and the short chain dehydrogenase PhqE from *phq* cluster suggests a reasonable pathway from L-isoleucine to β -methyl proline (Fig. 4). Similar to the partially identified biosynthesis of 4-methyl proline in cyanobacterial *Nostoc* sp.,⁶⁴ PhqE presumably oxidizes the terminally hydroxylated L-isoleucine (by an unknown enzyme) to the corresponding aldehyde. Spontaneous cyclization and dehydration would yield the 4-methyl pyrroline-5-carboxylic acid, which is then reduced by PhqD leading to the β -methyl proline precursor.

The presence of a C-terminal NAD(P)-dependent reductase domain in the bimodular paraherquamide NRPS (A-T-C-A-T-R) clearly indicates that the mechanism for dipeptide release by PhqB must be different from the final condensation domain of NotE (Fig. 3).⁵⁰ What likely occurs is that the PhqB R domain utilizes NADPH for hydride transfer to reduce the thioester bond of the T domain-tethered linear dipeptide to a hemithioaminal intermediate, which spontaneously cleaves the C-S bond to release the aldehyde product. Subsequently, the acid-activated aldehyde is intramolecularly trapped by the nucleophilic amine from the adjacent amino acid to form a hemiaminal intermediate, which then undergoes a spontaneous dehydration and double bond rearrangement leading to formation of the monooxopiperazine intermediate **16** (likely existing as the enol form) prior to all other biosynthetic steps. This hypothesis is in good agreement with previous observations^{65,66} that the dioxopiperazine analog of preparaherquamide (**17**) cannot be incorporated into **2** by *P. fellutanum* since all substrates for downstream enzymes should bear the monooxopiperazine ring system. In this scheme (Fig. 4), formation of the diene in **16** is achieved by a reductive process, as opposed to the $2e^-$ oxidation step proposed in the notoamide biosynthetic pathway (Fig. 3). If this is correct, in contrast to an oxidase (NotH/NotH' or NotD/NotD') proposed to be the Diels Alderase in notoamide biosynthesis, the reverse prenyltransferase (proposed to be PhqJ) might act as the scaffold for an IMDA reaction after introduction of the reverse prenyl group to **16**. In this proposed route, the terminal double bond of the isoprene group would become the dienophile to react with the azadiene in the prenyltransferase active site, thus resulting in formation of the [2.2.2] diazoctane intermediate **17**.

Following formation of **17**, the pyran ring formation is proposed to be installed by PhqA prenyltransferase (22% identical to NotC), PhqL (29% identical to NotG) and PhqH oxidoreductase (34% identical to NotD) (or PhqM P450 enzymes (15% identical to NotH)). The FMO PhqK (32% identical to NotI) is likely responsible for generation of the *spiro*-oxindole, and the *N*-methylation is likely mediated by the PhqN methyltransferase leading to the isolable natural product paraherquamide F^{38,67} (**18**). However, the order of these biosynthetic steps cannot be predicted without further *in vivo* genetic studies and/or *in vitro* biochemical analysis.

In late-stage paraherquamide biosynthesis, the third P450 monooxygenase PhqO is probably responsible for the C14 hydroxylation, transforming **18** to paraherquamide G^{38,67} (**19**), and paraherquamide E^{38,67} (**20**) to the final product **2**. However, expansion from the 6-membered ring pyran (in **18** and **19**) to the 7-membered dioxepin ring (in **2** and **20**) represents a poorly understood but intriguing process. Possibly, *phqC* that encodes a 2OG-Fe(II)-oxygenase is involved in this ring expansion, which is consistent with previous reports showing this class of enzyme functioning as an expandase.⁶⁸

Finally, the biosynthetic genes, including *phqI* as well as *phqM* (or *phqH*, the one uninvolved in the pyran ring formation), do not have a clearly prescribed role and appear to be redundant. This redundancy is currently being tested by gene knock-out studies in our laboratories.

Biosynthetic pathway of malbrancheamide (**3**)

Except for using L-proline instead of β -methyl proline as the starter unit, the biosynthetic route through premalbrancheamide (**21**) (Fig. 5) is proposed to parallel that of paraherquamide biosynthesis through **17** (Fig. 4). Mediated by NRPS MalG (A-T-C-A-T-R, 37% identical to PhqB) and prenyltransferase MalE (36%/34% identical to NotF/PhqJ), **21** is produced with its structure slightly different from **17** in lacking the C1 methyl group.

Subsequently, the halogenase MalA presumably chlorinates the C9 position (malbrancheamide numbering) first to afford the isolable natural product malbrancheamide B (**22**), which could be further chlorinated by MalA at C8 leading to the final product malbrancheamide (**3**). This putative pathway is partially supported by the previous feeding study showing that the ¹³C labeled **21** can be incorporated into **22** by *M. aurantiaca*.⁶⁹ Lack of observed ¹³C labeled **3** from the fermentation broth was interpreted to suggest that the second chlorination might be too slow to incorporate detectable levels of ¹³C material from **22** to **3**. Notably, the order of these two chlorinations seems unexchangeable since the C8-monochloro regioisomer of **22** (C9-monochlorinated) was not detected as a natural product despite considerable effort.⁴² It is also possible that the dichloro species, malbrancheamide, arises from a pre-halogenated tryptophan-based assembly.

Blast (<http://blast.ncbi.nlm.nih.gov/>) sequence analysis revealed significant homology of MalA to the family of flavin-dependent tryptophan halogenases.⁷⁰⁻⁷³ This may suggest two alternative malbrancheamide biosynthetic pathways. First, MalA could chlorinate tryptophan at C4 and C5 (tryptophan numbering) sequentially prior to being loaded onto the second T domain of MalG. Then, both monochlorinated and dichlorinated tryptophan could be processed by subsequent assembly enzymes, thereby respectively leading to **22** and **3** in parallel. Second, MalA might only monochlorinate the C4 position of tryptophan, resulting in **22**. Then, **22** is converted into **3** by either MalA or another unidentified halogenase that resides outside *mal*. To test these hypotheses, it would be the best to conduct *in vitro* functional analysis of purified MalA against selected substrates such as L-tryptophan and **22**. Alternatively, whether or not the ¹³C labeled **22** can be incorporated into **3** in an *in vivo* precursor feeding study would also provide useful information about the timing of the two chlorination steps in malbrancheamide biosynthesis.

According to the proposed malbrancheamide biosynthetic pathway (Fig. 5), only three enzymes are required to assemble the final product **3**. Inactivation of these seemingly redundant genes including *malB*, *malC*, and *malF* (Table 1) is currently underway. Interestingly, the MalC short chain dehydrogenase related to PhqE, which is presumed to participate in preparation of β -methyl proline starter unit in paraherquamide biosynthesis (see above), is present in the *mal* gene cluster although apparently unnecessary for malbrancheamide biosynthesis. This implies that *malC*, together with other redundant genes,

might be residuals from ancestral or a horizontally transferred gene cluster (e.g. one analogous to *phq*). The evolving biosynthetic gene cluster not only recruits new genes, but also eliminates or retains unused genes when facing a diverse living environment and selection pressure during its evolutionary history.²⁴

Recently, a novel malbrancheamide-type natural product named spiromalbramide (**23**) (Fig. 5) was isolated from a marine invertebrate-derived *Malbranchea graminicola* fungal strain.⁷⁴ This new derivative contains the *spiro*-oxindole moiety that is found in notoamides and paraherquamides, but is absent from malbrancheamides. Based on the comparative analysis of *not*, *not'*, *phq*, and *mal* gene cluster, we are now capable of predicting that an FMO gene homologous to *notI*, *notI'* or *phqK* should reside in the uncharacterized biosynthetic gene cluster of **23**. So far, the Solexa genome sequencing of *M. graminicola* has been completed. This prediction will be tested in the near future as soon as the biosynthetic gene cluster is mined and annotated from genome sequences.

Conclusion

The increasing pace of whole genome sequencing projects supported by a new generation of high throughput technologies have led to exponentially increased number of natural product biosynthetic gene clusters identified *in silico*. The accumulated knowledge based on previously characterized biosynthetic pathways and functionally defined biosynthetic enzymes, is enabling meaningful comparative analyses of new biosynthetic gene clusters. In turn, this is enabling an efficient approach to predict new biosynthetic pathways, propose enzyme candidates for unknown biosynthetic transformations, and to prioritize targets for focused genetic and biochemical research.

In principle, the shared genes from different clusters are responsible for assembling the common structural core among similar natural products. The cluster-specific gene products are presumed to modify these structures by a series of variant tailoring steps, thereby leading to structural diversification. However, it is noteworthy that the redundant genes and multifunctional genes could complicate comparative analysis of gene clusters. Therefore, conclusions can only be unambiguously drawn after genetic and/or biochemical confirmation of enzymatic activities.

Following these simple but logical principles, we performed a comparative analysis for four related gene clusters including *not*, *not'*, *phq*, and *mal*, based on the proposed complete biosynthetic pathways for (+)/(-)-notoamides, paraherquamides, and malbrancheamides with a biosynthetic enzyme assigned for each individual step (Fig. 3–5). For example, the function of the *not*-specific gene *notB* can be readily connected to the pathway specific transformation from notoamide E (**8**) to notoamide C (**9**) and D (**10**). This was recently confirmed by *in vitro* characterization of NotB FMO enzyme.⁵⁸

Furthermore, detailed comparative analysis resulted in nomination of the oxidases NotH and NotH' (or NotD and NotD'), and the prenyltransferases PhqJ and MalE as putative Diels-Alderas to catalyze the distinctive IMDA reactions for these pathways. Next, comparative functional analysis of these enzymes *in vitro* will enable us to test this long standing hypothesis regarding the existence of a Diels-Alderase in the biosynthesis of fungal indole alkaloids with the bicyclo[2.2.2]diazaoctane core. It is striking that Nature has conscripted two evolutionarily related gene cluster paradigms, to construct the novel bicyclo[2.2.2]diazaoctane ring system by vastly different mechanistic protocols (Figure 6). In one instance, for the notoamides, the net transformation from the NRPS-loaded dipeptide to the bicyclo[2.2.2]diazaoctane core, a net two-electron oxidation is required to reach the key, putative azadiene species required for the proposed IMDA construction. In the other,

the paraherquamide and malbrancheamide systems, the NRPS-loaded dipeptide substrate is cleaved in a net two-electron reduction, that we speculate cyclizes and dehydrates to the related (reduced) azadiene species for the homologous IMDA construction. This insight was most readily presented to us, by the analysis of the respective gene cluster annotations, and has provided a very satisfying level of corroboration with labeled precursor incorporation experiments that at first, seemed incongruous. We expect that the tremendous insights that the bioinformatics analyses have provided in these systems, will render understanding the possible biogenesis of these and related natural products more efficient, congruent and intellectually satisfying.

Supplementary Material

Refer to Web version on PubMed Central for supplementary material.

Acknowledgments

This work was supported by NIH grant R01 CA070375 (R.M.W. and D.H.S.) and the Hans W. Vahlteich Professorship (D.H.S.). Dr. James Cavalcoli of Center for Computational Medicine and Bioinformatics, University of Michigan is gratefully acknowledged for helpful discussions on genome assembly and bioinformatic analysis. We are also thankful to Drs. Brendan Tarrier, Christine Brennan, and Robert Lyons from University of Michigan DNA Sequencing Core for genome sequencing technical support and helpful suggestions.

References

1. Li JWH, Vederas JC. *Science*. 2009; 325:161. [PubMed: 19589993]
2. Newman DJ, Cragg GM. *J Nat Prod*. 2007; 70:461. [PubMed: 17309302]
3. Li R, Townsend CA. *Metab Eng*. 2006; 8:240. [PubMed: 16530442]
4. Baltz RH. *J Ind Microbiol Biotechnol*. 1998; 20:360.
5. Baba S, Abe Y, Suzuki T, Ono C, Iwamoto K, Nihira T, Hosobuchi M. *Appl Microbiol Biotechnol*. 2009; 83:697. [PubMed: 19277641]
6. Noh J-H, Kim S-H, Lee H-N, Lee SY, Kim E-S. *Appl Microbiol Biotechnol*. 2010; 86:1145. [PubMed: 20020285]
7. Strohl WR. *Metab Eng*. 2001; 3:4. [PubMed: 11162228]
8. Cane DE, Walsh CT, Khosla C. *Science*. 1998; 282:63. [PubMed: 9756477]
9. Walsh CT. *ChemBioChem*. 2002; 3:125. [PubMed: 11921390]
10. Sanchez C, Zhu L, Brana AF, Salas AP, Rohr J, Mendez C, Salas JA. *Proc Natl Acad Sci USA*. 2005; 102:461. [PubMed: 15625109]
11. Pollier J, Moses T, Goossens A. *Nat Prod Rep*. 2011; 28:1897. [PubMed: 21952724]
12. Que JL, Tolman WB. *Nature*. 2008; 455:333. [PubMed: 18800132]
13. Goff AL, Artero V, Jusselme B, Tran PD, Guillet N, Métayé R, Fihri A, Palacin S, Fontecave M. *Science*. 2009; 326:1384. [PubMed: 19965754]
14. Watts KT, Mijts BN, Schmidt-Dannert C. *Adv Synth Catal*. 2005; 347:927.
15. Xue Y, Zhao L, Liu H-w, Sherman DH. *Proc Natl Acad Sci USA*. 1998; 95:12111. [PubMed: 9770448]
16. Carlson JC, Fortman JL, Anzai Y, Li S, Burr DA, Sherman DH. *ChemBioChem*. 2010; 11:564. [PubMed: 20127927]
17. Kittendorf JD, Sherman DH. *Bioorg Med Chem*. 2009; 17:2137. [PubMed: 19027305]
18. Carlson JC, Li S, Gunatilleke SS, Anzai Y, Burr DA, Podust LM, Sherman DH. *Nat Chem*. 2011; 3:628. [PubMed: 21778983]
19. Zhang H, Boghigian BA, Armando J, Pfeifer BA. *Nat Prod Rep*. 2011; 28:125. [PubMed: 21060956]
20. Galm U, Shen B. *Expert Opin Drug Discov*. 2006; 1:409.

21. Tang L, Shah S, Chung L, Carney J, Katz L, Khosla C, Julien B. *Science*. 2000; 287:640. [PubMed: 10649995]
22. Cheng Q, Xiang L, Izumikawa M, Meluzzi D, Moore BS. *Nat Chem Biol*. 2007; 3:557. [PubMed: 17704772]
23. Balibar CJ, Howard-Jones AR, Walsh CT. *Nat Chem Biol*. 2007; 3:584. [PubMed: 17704773]
24. Gu L, Wang B, Kulkarni A, Geders TW, Grindberg RV, Gerwick L, Håkansson K, Wipf P, Smith JL, Gerwick WH, Sherman DH. *Nature*. 2009; 459:731. [PubMed: 19494914]
25. Anzai Y, Li S, Chaulagain MR, Kinoshita K, Montgomery J, Sherman DH. *Chem Biol*. 2008; 15:950. [PubMed: 18804032]
26. Galm U, Wendt-Pienkowski E, Wang L, Huang S-X, Unsinn C, Tao M, Coughlin JM, Shen B. *J Nat Prod*. 2011; 74:526. [PubMed: 21210656]
27. Péant B, LaPointe G, Gilbert C, Atlan D, Ward P, Roy D. *Microbiology*. 2005; 151:1839. [PubMed: 15941992]
28. Ryan KS. *PLoS One*. 2011; 6:e23694. [PubMed: 21876764]
29. Buntin K, Irschik H, Weissman KJ, Luxemburger E, Blöcher H, Müller R. *Chem Biol*. 2010; 17:342. [PubMed: 20416506]
30. Hawkins RD, Hon GC, Ren B. *Nat Rev Genet*. 2010; 11:476. [PubMed: 20531367]
31. Metzker ML. *Nat Rev Genet*. 2010; 11:31. [PubMed: 19997069]
32. Treangen TJ, Salzberg SL. *Nat Rev Genet*. 2012; 13:36. [PubMed: 22124482]
33. Shaffer C. *Nat Biotechnol*. 2007; 25:149. [PubMed: 17287734]
34. Schuster SC. *Nat Methods*. 2008; 5:16. [PubMed: 18165802]
35. Kato H, Yoshida T, Tokue T, Nojiri Y, Hirota H, Ohta T, Williams RM, Tsukamoto S. *Angew Chem Intl Ed*. 2007; 46:2254.
36. Greshock TJ, Grubbs AW, Jiao P, Wicklow DT, Gloer JB, Williams RM. *Angew Chem Intl Ed*. 2008; 47:3573.
37. Yamazaki M, Okuyama E, Kobayashi M, Inoue H. *Tetrahedron Lett*. 1981; 22:135.
38. Ondeyka JG, Goegelman RT, Schaeffer JM, Kelemen L, Zitano L. *J Antibiot*. 1990; 43:1375. [PubMed: 2272914]
39. Williams RM, Gao J, Tsujishima H, Cox RJ. *J Am Chem Soc*. 2003; 125:12172. [PubMed: 14519003]
40. Martinez-Luis S, Rodriguez R, Acevedo L, Gonzalez MC, Lira-Rocha A, Mata R. *Tetrahedron*. 2006; 62:1817.
41. Figueroa M, Gonzalez MC, Mata R. *Nat Prod Res*. 2008; 22:709. [PubMed: 18569711]
42. Miller KA, Welch TR, Greshock TJ, Ding Y, Sherman DH, Williams RM. *J Org Chem*. 2008; 73:3116. [PubMed: 18345688]
43. Ding Y, deWet JR, Cavalcoli J, Li S, Greshock TJ, Miller KA, Finefield JM, Sunderhaus JD, McAfoos TJ, Tsukamoto S, Williams RM, Sherman DH. *J Am Chem Soc*. 2010; 132:12733. [PubMed: 20722388]
44. Williams RM, Cox RJ. *Acc Chem Res*. 2003; 36:127. [PubMed: 12589698]
45. Stocking EM, Sanz-Cervera JF, Unkefer CJ, Williams RM. *Tetrahedron*. 2001; 57:5303.
46. Stocking EM, Williams RM. *Angew Chem Intl Ed*. 2003; 42:3078.
47. Sunderhaus JD, Sherman DH, Williams RM. *Isr J Chem*. 2011; 51:442. [PubMed: 21818159]
48. Grubbs AW, Artman GDI, Tsukamoto S, Williams RM. *Angew Chem Intl Ed*. 2007; 46:2257.
49. Greshock TJ, Grubbs AW, Tsukamoto S, Williams RM. *Angew Chem Intl Ed*. 2007; 46:2262.
50. Keating TA, Ehmann DE, Kohli RM, Marshall CG, Trauger JW, Walsh CT. *ChemBioChem*. 2001; 2:99. [PubMed: 11828432]
51. Steffan N, Grundmann A, Afiyatullo S, Ruan H, Li S-M. *Org Biomol Chem*. 2009; 7:4082. [PubMed: 19763315]
52. Hausinger RP. *Crit Rev Biochem Mol Biol*. 2004; 39:21. [PubMed: 15121720]
53. Birch AJ, Wright JJ. *J Chem Soc Chem Commun*. 1969:644.
54. Li S-M. *J Antibiot*. 2011; 64:45. [PubMed: 21063425]

55. Kato N, Suzuki H, Takagi H, Takeya H, Uramoto M, Usui T, Takahashi S, Sugimoto Y, Osada H. *Chem Bio Chem*. 2009; 10:920.
56. Steyn PS. *Tetrahedron Lett*. 1971; 12:3331.
57. Tsukamoto S, Kato H, Greshock TJ, Hirota H, Ohta T, Williams RM. *J Am Chem Soc*. 2009; 131:3834. [PubMed: 19292484]
58. Li S, Finefield JM, Sunderhaus JD, McAfoos TJ, Williams RM, Sherman DH. *J Am Chem Soc*. 2012; 134:788. [PubMed: 22188465]
59. Oliynyk M, Stark CBW, Bhatt A, Jones MA, Hugher-Thomas ZA, Wilkinson C, Oliynyk Z, Demydchuk Y, Staunton J, Leadlay PF. *Mol Microbiol*. 2003; 49:1179. [PubMed: 12940979]
60. Qian-Cutrone J, Huang S, Shu YZ, Vyas D, Fairchild C, Menendez A, Krappitz K, Dalterio R, Klohr SE, Gao Q. *J Am Chem Soc*. 2002; 124:14556. [PubMed: 12465964]
61. Finefield JM, Kato H, Greshock TJ, Sherman DH, Tsukamoto S, Williams RM. *Org Lett*. 2011; 13:3802. [PubMed: 21714564]
62. Authrine C, Gloer JB. *J Nat Prod*. 1996; 59:1093. [PubMed: 8946752]
63. Stocking EM, Sanz-Cervera JF, Williams RM. *J Am Chem Soc*. 2000; 122:1675.
64. Luesch H, Hoffmann D, Hevel JM, Becker JE, Golakoti T, Moore RE. *J Org Chem*. 2002; 68:83. [PubMed: 12515465]
65. Ding Y, Grüschow S, Greshock TJ, Finefield JM, Sherman DH, Williams RM. *J Nat Prod*. 2008; 71:1574. [PubMed: 18754595]
66. Stocking EM, Sanz-Cervera JF, Williams RM. *Angew Chem Intl Ed*. 2001; 40:1296.
67. Liesch JM, Wichmann CF. *J Antibiot*. 1990; 43:1380. [PubMed: 2272915]
68. Hewitson KS, Granatino N, Welford RWD, McDonough MA, Schofield CJ. *Phil Trans R Soc A*. 2005; 363:807. [PubMed: 15901537]
69. Ding Y, Greshock TJ, Miller KA, Sherman DH, Williams RM. *Org Lett*. 2008; 10:4863. [PubMed: 18844365]
70. vanPée KH, Patallo EP. *Appl Microbiol Biotechnol*. 2006; 70:631. [PubMed: 16544142]
71. Zeng J, Zhan J. *Chem Bio Chem*. 2010; 11:2119.
72. Neumann CS, Walsh CT, Kay RR. *Proc Natl Acad Sci USA*. 2010; 107:5798. [PubMed: 20231486]
73. Dong C, Flecks S, Unversucht S, Haupt C, vanPée KH, Naismith JH. *Science*. 2005; 309:2216. [PubMed: 16195462]
74. Watts KR, Loveridge ST, Tenney K, Media J, Valeriotte FA, Crews P. *J Org Chem*. 2011; 76:6201. [PubMed: 21682275]

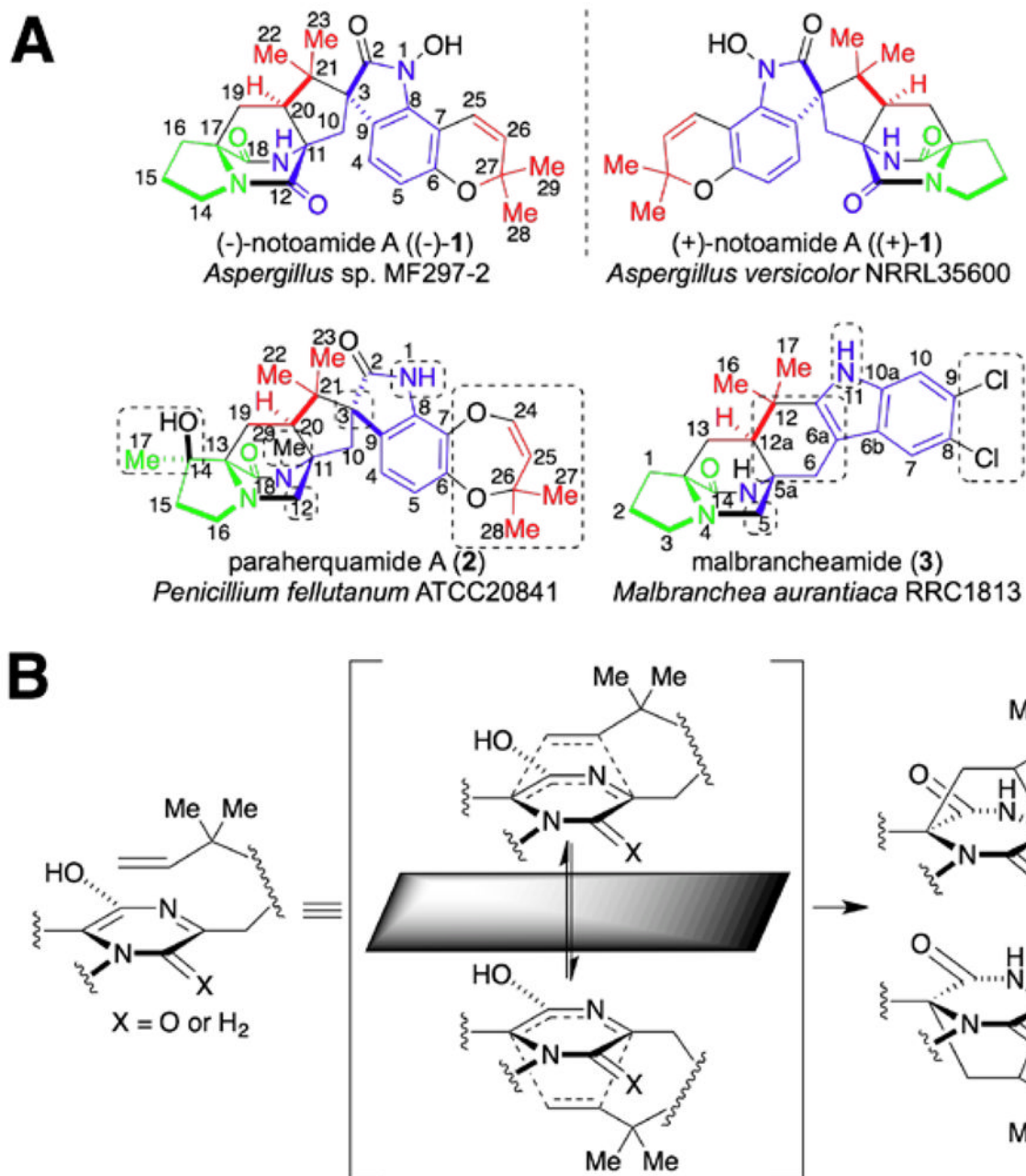


Figure 1.
 (A) Structures of (±)-notoamide A ((±)-1), paraherquamide A (2), and malbrancheamide (3). The unique structural features in 2 and 3 compared to 1 are highlighted in dashed boxes; (B) Proposed formation of the antipodal bicyclo[2.2.2]diazaoctane ring systems.

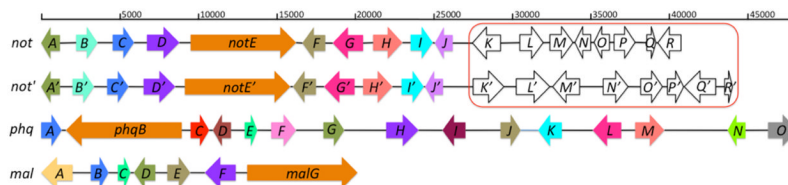


Figure 2.

The (–)-notoamide A (*not*), (+)-notoamide A (*not'*), paraherquamide (*phq*), and malbrancheamide (*mal*) biosynthetic gene clusters identified from genome sequencing and bioinformatic mining of *Aspergillus* sp. MF297-2, *Aspergillus versicolor* NRRL35600, *P. fellutanum* ATCC20841, and *M. aurantiaca* RRC1813, respectively. Homology of open reading frames across gene clusters is shown by same colored arrows. The *not* and *not'* genes in the red box are unlikely involved in notoamide biosynthesis.

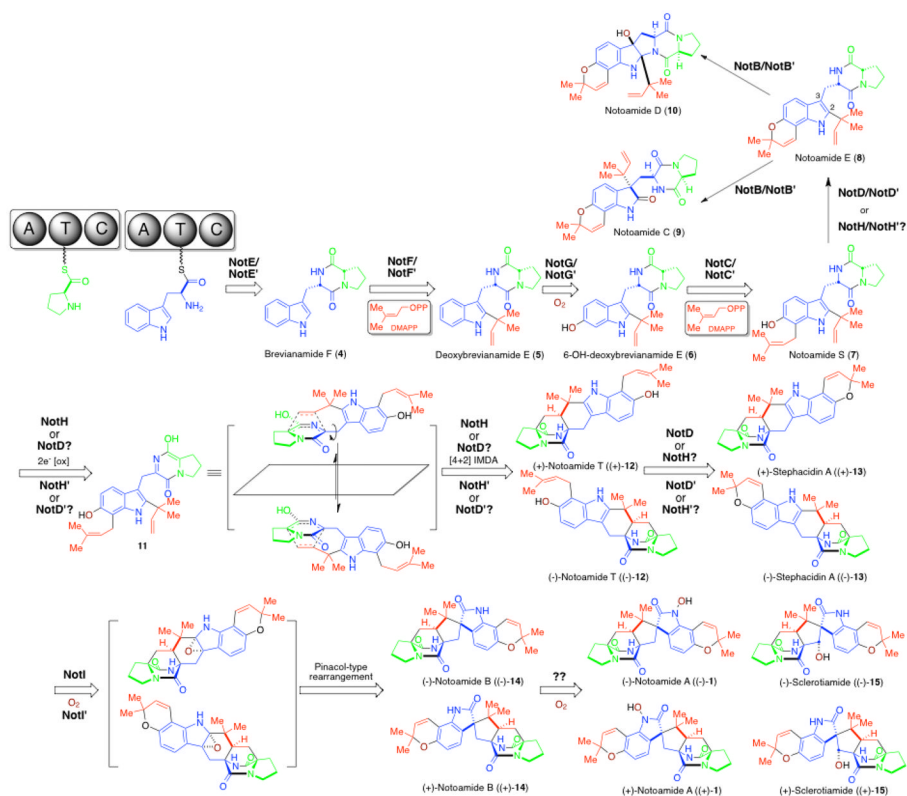


Figure 3.
Proposed biosynthetic pathway for antipodal notoamide metabolites.

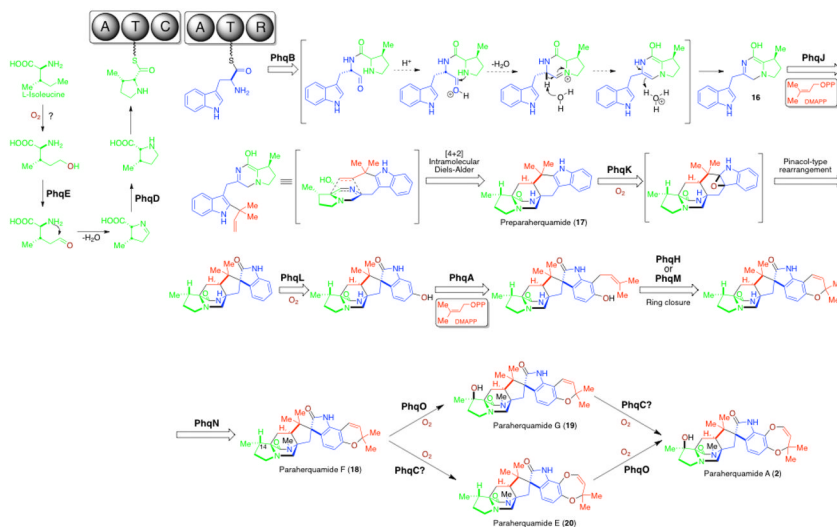


Figure 4.
Proposed biosynthetic pathway for paraherquamide A.

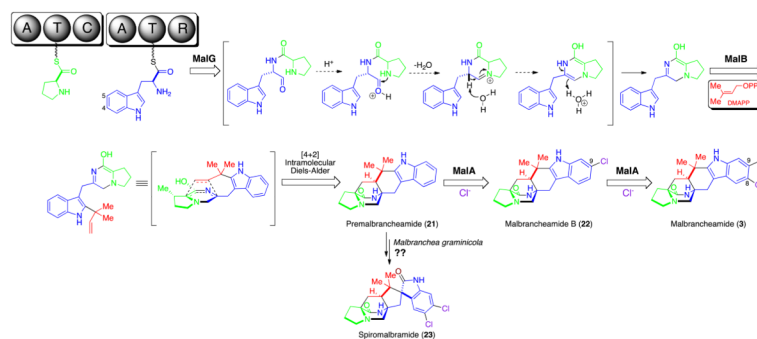


Figure 5.
Proposed biosynthetic pathway for malbrancheamide natural products.

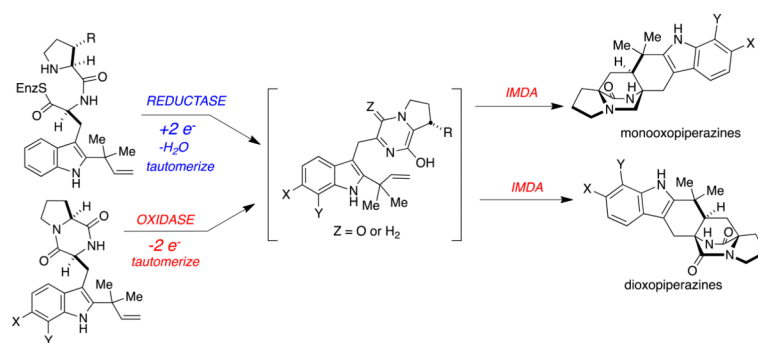


Figure 6. Summary of divergent NRPS strategies that culminate in the formation of structurally related bicyclo[2.2.2]diazaoctane ring systems in distinct oxidation states.

Table 1

Comparative analysis* of gene clusters of *not*, *not'*, *phq*, and *mal*

Not proteins (AA)	Function	Not' proteins (AA)	Function (%identity to corresponding Not protein)	Phq proteins (AA)	Function (%identity to corresponding Not protein)	Mal proteins (AA)	Function (%identity to corresponding Not/Phq protein)
NotA (339)	Negative regulator	NotA' (334)	Negative regulator (70% NotA)	PhqA (405)	Prenyltransferase (22% NotC)	MalA (667)	Halogenase (---)
NotB (456)	FAD monooxygenase	NotB' (455)	FAD monooxygenase (88% NotB)	PhqB (2449)	NRPS [A-T-C-A-T-R] (26% NotE)	MalB (369)	Prenyltransferase (28% NotC/34% PhqA)
NotC (427)	Prenyltransferase	NotC' (426)	Prenyltransferase (87% NotC)	PhqC (353)	2OG-Fe(II)-oxygenase (---)	MalC (264)	Short chain dehydrogenase (---52% PhqE)
NotD (621)	Oxidoreductase	NotD' (612)	Oxidoreductase (80% NotD)	PhqD (322)	Pyroline-5-carboxylate reductase (---)	MalD (336)	Negative regulator (36% NotA/55% PhqG)
NotE (2241)	NRPS [A-T-C-A-T-C]	NotE' (2225)	NRPS [A-T-C-A-T-C] (79% NotE)	PhqE (265)	Short chain dehydrogenase (---)	MalE (438)	Prenyltransferase (36% NotF/34% PhqJ)
NotF (453)	Prenyltransferase	NotF' (435)	Prenyltransferase (79% NotF)	PhqF (411)	Efflux pump (18% NotK)	MalF (590)	Oxidoreductase (37% NotD/39% PhqH)
NotG (544)	P450 monooxygenase	NotG' (544)	P450 monooxygenase (87% NotG)	PhqG (338)	Negative regulator (34% NotA)	MalG (2345)	NRPS [A-T-C-A-T-R] (27% NotE/37% PhqB)
NotH (502)	P450 monooxygenase	NotH' (499)	P450 monooxygenase (84% NotH)	PhqH (602)	Oxidoreductase (34% NotD)		
NotI (434)	FAD monooxygenase	NotI' (433)	FAD monooxygenase (85% NotI)	PhqI (462)	Prenyltransferase (---)		
NotJ (371)	Unknown	NotJ' (362)	Unknown (80% NotJ)	PhqJ (406)	Prenyltransferase (32% NotF)		
NotK (564)	Efflux pump	NotK' (577)	Efflux pump (14% NotK)	PhqK (459)	FAD monooxygenase (32% NotI)		
NotL (484)	Transcriptional activator	NotL' (620)	Transcriptional factor (15% NotL)	PhqL (563)	P450 monooxygenase (29% NotG)		
NotM (402)	Unknown	NotM' (454)	Unknown (---)	PhqM (536)	P450 monooxygenase (15% NotH)		
NotN (340)	Dehydrogenase	NotN' (416)	Unknown (---)	PhqN (326)	Methyltransferase		
NotO (331)	Short-chain dehydrogenase	NotO' (462)	Unknown (---)	PhqO (451)	P450 monooxygenase (---)		

\$watermark-text

\$watermark-text

\$watermark-text

Not proteins (AA)	Function	Not' proteins (AA)	Function (%identity to corresponding Not protein)	Phq proteins (AA)	Function (%identity to corresponding Not protein)	Mal proteins (AA)	Function (%identity to corresponding Not/Phq protein)
NotP (322)	Unknown	NotP' (292)	Unknown (∅)				
NotQ (152)	Unknown	NotQ' (506)	Transcription factor				
NotR (461)	Transcriptional coactivator	NotR' (172)	Unknown				

* Genes were predicted using the FGENSEH-M tool from <http://www.softberry.com>; Functions of gene products were predicted using BLAST search

∅ Homology cannot be calculated due to unrelatedness